

Analysis of Factors Affecting the Pigging Effect

Junlin Li, Yujia Li

School of Mechatronic Engineering, Southwest Petroleum University, and the Oil and Gas Equipment Technology Science and Technology Information Resource Sharing Service Platform of Sichuan Province, Chengdu 610500, China

Abstract: In order to ensure production and life safety in the process of oil and gas production, it is necessary to regularly perform pigging operations on pipelines. The fluid-solid coupling effect between the pig and pipeline impurities is complex, and theoretical methods are difficult to solve. Related experimental research is costly and experimental data is difficult to obtain. In order to further explore the factors affecting the cleaning effect of pigs in bi-metal composite pipes, this paper introduces fluid-solid coupling and uses the CEL method to establish a fluid-solid coupling model for the pig, pipeline impurities, and pipeline. The cleaning effect of the pipeline impurities is analyzed in terms of the shape, interference fit amount, and speed of the pig.

Keywords: Pigging effect; fluid-structure interaction; pig shape; interference amount; pig speed.

1. Introduction

In the transportation of oil and gas pipelines, high-sulfur gas field pipelines can generate natural gas hydrates and sulfur deposition due to transportation methods and other factors. These phenomena can cause pipeline blockages and even serious safety problems, posing a threat to people's lives and production. Currently, for the problem of natural gas hydrates in pipelines, the main treatments include adding natural gas hydrate inhibitors, controlling metering temperature, and pigging operations. For the problem of sulfur deposition, the main treatments include adding sulfur solvents, heating, optimizing pipeline system process parameters, and pigging operations[1][2][3].

Pigs were first used in the 1870s but only came of age in the 1940s with the construction of major pipelines[4]. Short pointed out in a report that although there have been many practical applications and accumulated experience in the engineering of cleaning devices, it is difficult to choose the appropriate type solely based on this[5]. Lino et al. conducted about 800 cleaning experiments on a test loop, but did not obtain any data of significant value for reference[6]. Mendes et al. studied for the first time the motion law of the cleaning device, and found that if there is a gap between the cleaning device and the inner wall of the pipeline, the fluid will enter the gap under the driving of the pressure difference before and after the cleaning device, which will affect the interaction between the pipeline wall and the cleaning device[7]. Wang et al[8]. and Wang Wenda[9] designed an experimental device to simulate the removal of oil-wax mixtures indoors. They tested the force required to peel off wax deposits under different conditions of clearers' hardness and obtained an empirical formula for the force required to peel off wax deposits. However, because the formula is purely empirical, this method has not been widely used. In the research process, it was found that the interference fit design has a crucial influence on the normal operation of the cleaning device. If the interference fit is too large, it may cause the cleaning device to jam; if the interference fit is too small, it will affect the cleaning effect[10].

The operation of the pipeline cleaning tool in the pipeline is a type of fluid-structure interaction behavior. Some scholars use CFD method to solve the fluid-solid coupling between the cleaning device and the fluid medium. Borregales et al. used

the CFD method to establish a two-dimensional flow field model of the cleaning pig, and analyzed the motion state of the cleaning pig during the launch process using dynamic mesh technology[11]. Parilli et al. used the CFD software CFX to establish a 3D model of the cleaning pig, analyzed the operation state of the cleaning pig in the pipeline, and analyzed the distribution of the flow field inside the pipeline. In addition, they also verified the accuracy of the simulation method by comparing it with experimental results[12][13].

However, these studies did not investigate the factors that affect the cleaning effectiveness of pigs. This article takes the polyurethane cleaning tool and its corresponding pipeline as the research object, establishes an elastic mechanics model, and solves its interference fit. For the polyurethane material used in the cleaning tool, the Mooney-Rivlin model is adopted and the relevant parameters are obtained through tensile tests. The CEL method is used to simulate the fouling on the inner wall of the pipeline and analyze the cleaning effect of the cleaning tool under different factors.

2. CEL Algorithm

During the pipe cleaning process, the pigs undergo large deformations of hyperelastic materials, as well as nonlinearities in material, geometry, and contact, and flow-structure coupling. Traditional finite element and computational fluid dynamics methods have difficulty effectively simulating this complex process. The CEL algorithm can effectively combine the advantages of the two methods mentioned above, and can simulate the entire process of the cleaning device operating in the pipeline.

2.1. CEL algorithm introduction

The traditional finite element method using the Lagrangian algorithm can accurately describe the deformation of materials, while the CFD method is mostly used to describe fluids[14]. The use of traditional finite element methods cannot introduce fluid effects, while the use of CFD methods cannot consider the contact between the cleaning device and the pipeline. Therefore, an effective method is needed to simulate the complex mechanical behavior of the cleaning device in the pipeline. The Coupled Eulerian-Lagrangian (CEL) algorithm, proposed by Noh WF[15], combines the advantages of the Lagrangian and Eulerian algorithms. In the analysis process using the CEL algorithm, a Lagrangian

region for describing solids and an Eulerian region for describing fluids are established separately. They are combined together by assembly, and the initial distribution state of the material in the Eulerian region is defined. During the calculation process, the exchange of force, displacement, and other information between the two regions is performed through the contact established between them, and the distribution state of the material in the Eulerian region is updated. In this study, the Lagrangian method is used to describe the behavioral characteristics of the cleaning device and pipeline, while the Eulerian method is used to describe the movement of impurities in the pipeline.

2.2. The Fluid Control Equations

In the CEL algorithm, the Eulerian volume fraction (EVF) method is used to determine the material boundary in the Eulerian domain[16]. The material in the Eulerian domain has relative independence between the material and the Eulerian node, and the distribution of the fluid material in the Eulerian element is determined by the EVF of the material in the Eulerian element. When the Eulerian element is filled with material, EVF=1; when there is no material in the Eulerian element, EVF=0; when the material only fills part of the element, the ratio of the volume of the element filled with material is calculated according to the method shown in Figure 1 to represent the current EVF of the element.

0.0	0.0	0.0	0.0	0.0	0.0
0.0	0.32	0.91	0.91	0.32	0.0
0.0	0.91	1.0	1.0	0.91	0.0
0.0	0.91	1.0	1.0	0.91	0.0
0.0	0.91	0.91	0.91	0.32	0.0
0.0	0.0	0.0	0.0	0.0	0.0

Figure 1. EVF

Based on the material properties of the studied fluid medium, this paper uses the Mie-Gruneisen equation of state in the linear U_s - U_p Hugoniot form from the EOS method to describe the state of the fluid medium. It assumes that the pressure p is only a function of the density ρ , and its energy equation can be solved through the continuity equation and momentum equation[17]. In the CEL method used in this paper, the Mie-Gruneisen equation of state is:

$$p - p_H = \Gamma_\rho (E_m - E_H) \quad (1)$$

In this equation, p_H represents Hugoniot pressure, which is usually obtained by curve fitting, E_H represents specific internal energy, and the Hugoniot pressure p_H and specific internal energy E_H have a functional relationship with density ρ . Γ represents the Gruneisen ratio, also known as the phonon, and its expression is:

$$\Gamma = \Gamma_0 \frac{\rho_0}{\rho} \quad (2)$$

The equation is as follows: where Γ_0 is the initial Gruneisen ratio, ρ_0 is the material's reference density, and the relationship between Hugoniot pressure p_H and specific internal energy E_H is given by:

$$E_H = \frac{p_H \eta}{2\rho_0} \quad (3)$$

In the equation, η is the nominal volumetric strain. Substituting Γ and E into equation (1) and simplifying, we can obtain:

$$p = p_H \left(1 - \frac{\Gamma_0 \eta}{2}\right) + \Gamma_0 \rho_0 e \quad (4)$$

The expression for p_H , which satisfies the Hugoniot curve fitting, is:

$$p_H = \frac{\rho_0 c_0^2 \eta}{(1 - s\eta)^2} \quad (5)$$

where c_0 and s are linear parameters between the fluid shock velocity U_s and the fluid particle velocity U_p , and the relationship between U_s and U_p is:

$$U_s = c_0 + sU_p \quad (6)$$

Substituting equation (5) into equation (4), the linear expression of U_s - U_p is obtained as follows:

$$p = \frac{\rho_0 c_0^2 \eta}{(1 - s\eta)^2} \left(1 - \frac{\Gamma_0 \eta}{2}\right) + \Gamma_0 \rho_0 e \quad (7)$$

The continuity equation and momentum equation in the CEL method are:

$$\frac{D\rho}{Dt} + \rho \nabla \cdot \frac{Dd}{Dt} = 0 \quad (8)$$

$$\rho \frac{D^2 d}{Dt^2} + \rho g - \nabla \cdot \sigma = 0 \quad (9)$$

Where the Cauchy stress tensor $\sigma = -pI + \sigma_{dev}$ is obtained from the EOS state equation, and $v = Dd/Dt$ is defined by the Newtonian shear stress.

3. Establishment of Fluid-structure Interaction Model

3.1. Geometric model

The geometry model established in this paper is shown in Figure 2, Where D_e is the Eulerian outer diameter, with a value of 301 mm; d is the inner diameter of the pipeline, with a value of 295 mm. Due to the special nature of the CEL method, the Eulerian domain for describing fluids needs to wrap around the Lagrangian domain for describing solids. The dashed region in the geometry model represents the Eulerian domain in the fluid-structure coupling model.

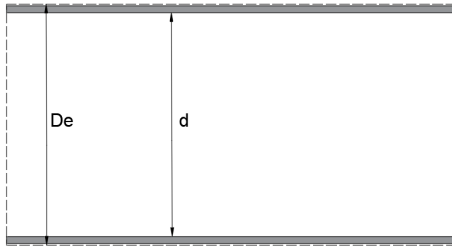


Figure 2. Geometry model

3.2. Finite element model

The fluid-structure coupling model established in this paper is shown in Figure 3. The red part represents the impurity area with a thickness of 20mm, and the blue part represents the impurity-free area inside the pipe. The Lagrangian description method in the CEL method is used for the Lagrangian domain, and the Eulerian description method is used for the fluid domain. The C3D8 mesh is used for the Lagrangian domain, and the EC3D8 mesh is used for the Eulerian domain. The scraper is described using the Mooney-Rivlin model, with $C10=0.34375$ and $C01=1.289$. An oil-wax mixture is used as the impurity medium, and the linear Us-Up Hugoniot form of the Mie-Gruneisen equation of state in the EOS method is used for the description. The selected impurity medium is an oil-wax mixture with density $\rho = 890kg/cm^3$, viscosity $\nu = 260mPa \cdot s$, Gruneisen constant $\Gamma = 0$, and Us-Up linear relationship parameters = 0. The two ends of the pipe are completely constrained, and different speeds and interference amounts are set for the scraper to simulate and analyze using dynamic method.

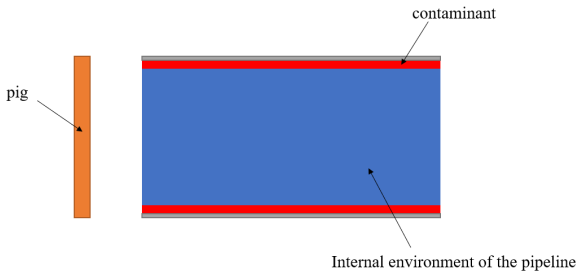
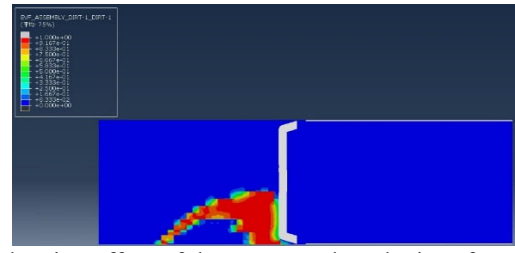


Figure 3. Internal environment of the pipeline

4. Influence of Pig Shape and Interference Fit on Pigging Effect

The finite element simulation was conducted under the condition of 22°C. After data processing, Figure 4 shows the cleaning effect of the scraper pig at different interference fits. When the interference fit is 1%, the scraper pig can remove the impurities completely and peel them off from the pipe wall, leaving no impurities in the pipeline. The cleaning effect is the best. When the interference fit is 2%, the cleaning effect is not different from that of 1%, and the impurities on the pipe wall are completely removed with no residue left in the pipeline, indicating an ideal cleaning effect. As the interference fit of the scraper pig has already achieved the best cleaning effect at 1% and there is no difference in cleaning effect between 2% and 1%, there is no need to simulate the cleaning effect of the scraper pig with interference fits of 3% and 4%. Therefore, when using a scraper pig for cleaning operations, an interference fit of 1% can achieve the best cleaning effect.



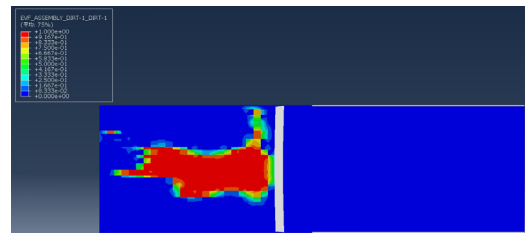
(a) Cleaning effect of the scraper when the interference fit is 1%



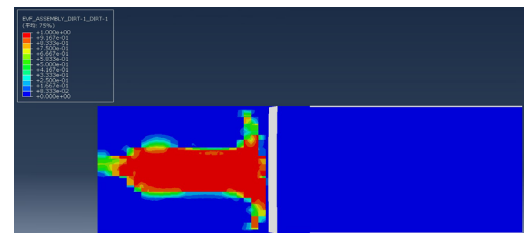
(b) Cleaning effect of the scraper when the interference fit is 2%

Figure 4. Cleaning Effect of Conical Scraper with Different Overlap Clearances

The finite element simulation was carried out under the condition of 22°C. After data processing, Figure 5 shows the cleaning effect of the straight plate cleaner under different interference fits. When the interference fit is 1%, the cleaner can completely remove impurities from the pipe wall without any impurities remaining in the pipeline, and the cleaning effect is the best. When the interference fit is 2%, there is no difference in cleaning effect compared to when the interference fit is 1%, and the pipe wall impurities are completely removed, and there are no impurities remaining inside the pipeline, indicating that the cleaning effect is ideal. Since the interference fit of the cleaner has already achieved the best effect when it is 1%, and there is no difference in cleaning effect between the interference fits of 1% and 2%, there is no need to simulate the cleaning effect of interference fits of 3% and 4%. Therefore, when selecting the straight plate cleaner for cleaning operations, an interference fit of 1% can achieve the best cleaning effect.



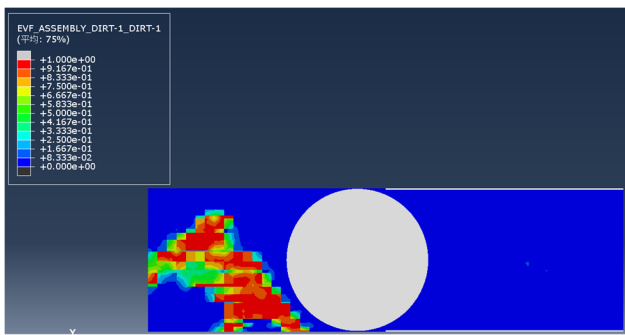
(a) Cleaning effect of the scraper when the interference fit is 1%



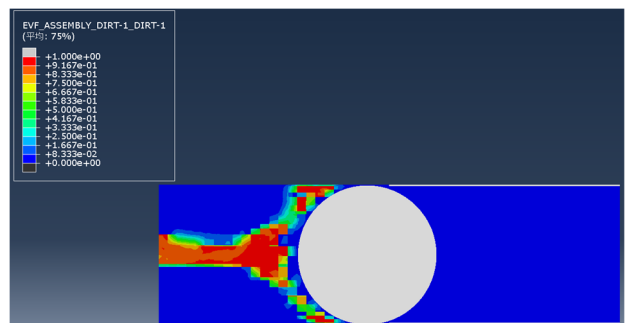
(b) Cleaning effect of the scraper when the interference fit is 2%

Figure 5. Cleaning effects of the straight blade pig at different interference ratios

Finite element simulation was conducted under the condition of 22°C. After data processing, Figure 6-6 shows the cleaning effect of the spherical cleaning tool at different interference fits. When the interference fit is 1%, the cleaning tool removes impurities comprehensively, can completely peel off impurities on the pipe wall, and there is no impurity residue inside the pipeline, achieving the best cleaning effect. When the interference fit is 2%, the cleaning effect is no different from that when the interference fit is 1%, and the impurities on the pipe wall are completely removed, and there is no impurity residue inside the pipeline, achieving an ideal cleaning effect. Since the cleaning tool has reached the best effect when the interference fit is 1%, and there is no difference in the cleaning effect when the interference fit is 2% compared to when the interference fit is 1%, it is not necessary to simulate the cleaning effect of the cleaning tool with interference fits of 3% and 4%. Therefore, when using a spherical cleaning tool for cleaning operations, a cleaning tool with an interference fit of 1% can achieve the best cleaning effect.



(a) Cleaning effect of the scraper when the interference fit is 1%



(b) Cleaning effect of the scraper when the interference fit is 2%

Figure 6. Clearing Effect of Spherical Tube Pig at Different Interference Fits

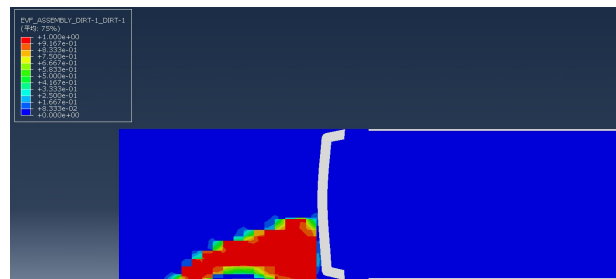
From the above results, it can be clearly seen that when using the cup-shaped, flat plate, and spherical cleaning tools for cleaning pipelines, the impurities on the pipe wall are completely removed with a cleaning tool interference fit of 1%, and the cleaning effect with a cleaning tool interference fit of 2% is identical to that with a cleaning tool interference fit of 1%. Therefore, when selecting the cup-shaped, flat plate, or spherical cleaning tool, an interference fit of 1% can achieve the best cleaning effect.

5. The Impact of Pig Speed on Pipeline Cleaning Performance

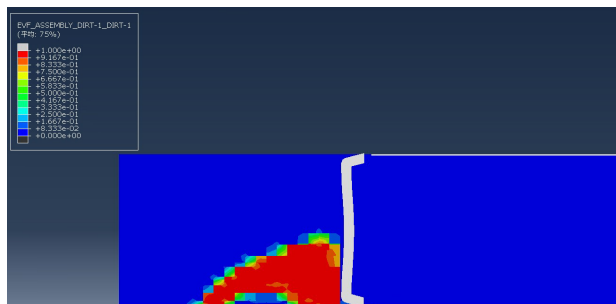
When performing pigging operations on pipelines, the

cleaning effect and efficiency of different types of pigs may be affected by their operating speed. In the following experiments, pigs of the cup type, the disc type, and the sphere type were used at different speeds (2m/s, 4m/s, and 6m/s) with an interference fit of 1% to clean the pipeline.

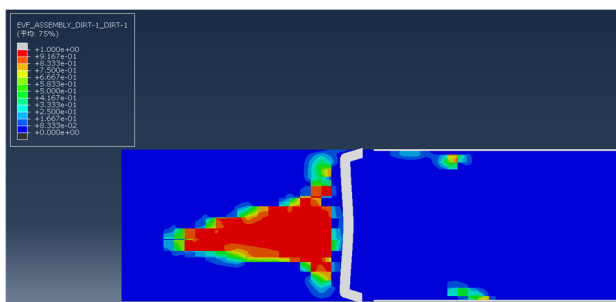
The finite element simulation was conducted at 22°C. After data processing, Figure 7 shows the cleaning effect of the cup-type pig at different speeds. At a speed of 2m/s, the cup-type pig removed all impurities completely from the pipe wall, and there was no residual impurities in the pipeline, resulting in the best cleaning effect. At a speed of 4m/s, the cleaning effect was not significantly different from that at a speed of 2m/s. The pipe wall impurities were completely removed, and there was no impurity residue in the pipeline, resulting in an ideal cleaning effect. At a speed of 6m/s, due to the excessively high speed of the cup-type pig, the cup and the pipe wall impurities did not fully contact, and most of the impurities were detached from the pipe wall. However, some impurities remained uncleared, which required subsequent cleaning processes or increasing the number of sealing discs of the cup-type pig to be effectively removed. Therefore, when using the cup-type pig for cleaning operations, the optimal cleaning effect and efficiency can be achieved at a speed of 4m/s.



(a) Cleaning effect of the pig at a speed of 2m/s



(b) Cleaning effect of the pig at a speed of 4m/s

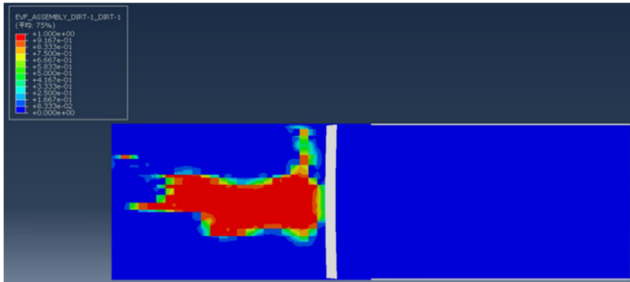


(c) Cleaning effect of the pig at a speed of 6m/s

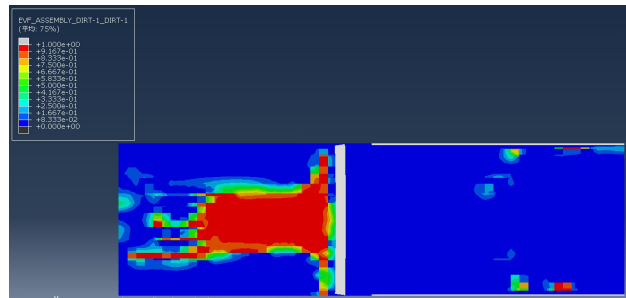
Figure 7. Cleaning effect of the pig with different operating speeds for the cup-type pig.

Finite element simulation was conducted under the condition of 22°C. After data processing, Figure 6-8 shows the cleaning effect of the straight blade pig at different speeds.

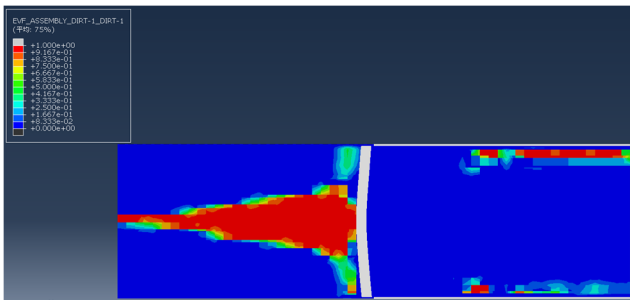
When the pig speed is 2m/s, the pig can remove impurities completely from the pipe wall without any impurities remaining inside the pipeline, resulting in the best cleaning effect. When the pig speed is 4m/s and 6m/s, due to the excessively fast speed, the contact between the straight blade and the impurities on the pipe wall is insufficient. Most of the impurities can be removed from the pipe wall, but some impurities still remain inside the pipeline and require further cleaning procedures to be removed. Therefore, when using the straight blade pig for pipeline cleaning, the optimal cleaning effect and efficiency can be achieved by setting the pig speed to 2m/s.



(a) Cleaning effect of the pig at a speed of 2m/s



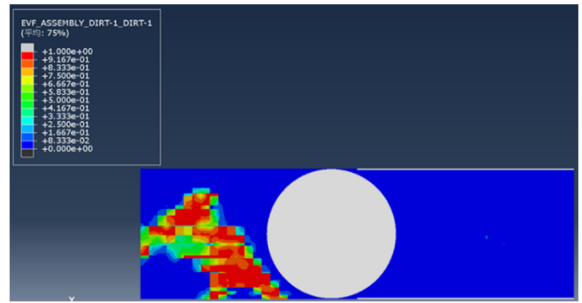
(b) Cleaning effect of the pig at a speed of 4m/s



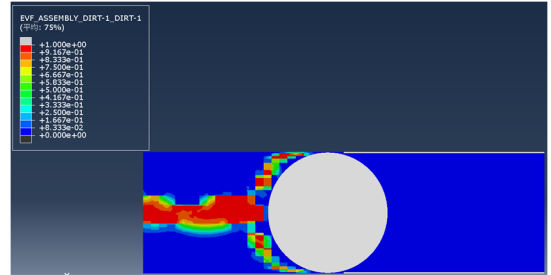
(c) Cleaning effect of the pig at a speed of 6m/s

Figure 8. The cleaning effect of a straight pig at different running speeds

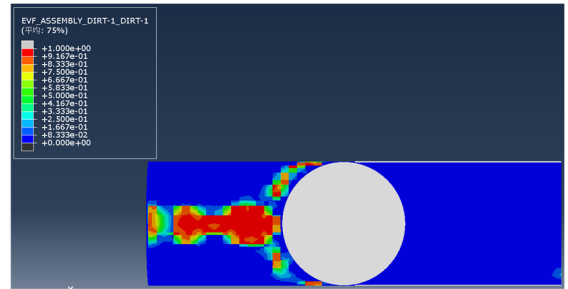
The finite element simulation was conducted under the condition of 22°C. After data processing, Fig. 6-9 shows the cleaning effect of the spherical cleaning device at different speeds. When the cleaning speed of the cleaning device is 2m/s, 4m/s, and 6m/s, the cleaning effect is the same. The cleaning device can completely strip impurities from the pipe wall and no impurities are left inside the pipeline. The cleaning effect is the best. Therefore, when using a spherical cleaning device for cleaning operations, the optimal cleaning speed is 6m/s.



(a) Cleaning effect of the pig at a speed of 2m/s



(b) Cleaning effect of the pig at a speed of 4m/s



(c) Cleaning effect of the pig at a speed of 6m/s

Figure 9. Cleaning effect of spherical pig at different operating speeds.

Figure 10 shows a comparison of the residual amount of debris on the pipe wall after cleaning with different shapes and interference fits of cleaning tools. It can be clearly seen from the figure that when using a bowl-shaped cleaning tool for cleaning, the residual debris on the pipe wall decreases with the increase of the interference fit. The best cleaning effect is achieved when the interference fit of the cleaning tool is 1%. When using a straight plate cleaning tool or a spherical cleaning tool for cleaning, the cleaning effect is the same when the interference fit is 1%, and the cleaning effect is the same as that when the interference fit is 2%. Therefore, if the cleaning tool shape is selected as a bowl-shaped cleaning tool, the cleaning tool speed setting of 4m/s can achieve the best cleaning effect and efficiency. If the cleaning tool shape is selected as a straight plate cleaning tool, the cleaning tool speed setting of 2m/s can achieve the best cleaning effect and efficiency. If the cleaning tool shape is selected as a spherical cleaning tool, the cleaning tool speed setting of 6m/s can achieve the best cleaning effect and efficiency.

6. Summary

This paper explores the factors affecting the cleaning effect of pipeline cleaners and introduces the fluid-structure coupling effect. The CEL method is used to establish a fluid-structure coupling model of the pipeline cleaner, pipeline impurities, and pipeline. The cleaning effect of pipeline impurities under different shapes, interference fit, and speeds of pipeline cleaners is analyzed. The research shows that

when using a concave bowl-shaped pipeline cleaner for cleaning operations, the recommended interference fit is 1%, and the recommended cleaning speed is 4m/s. When using a straight plate-shaped pipeline cleaner for cleaning operations, the recommended interference fit is 1%, and the recommended cleaning speed is 2m/s. When using a spherical pipeline cleaner for cleaning operations, the recommended interference fit is 1%, and the recommended cleaning speed is 6m/s. Considering the three factors of pipeline cleaner shape, interference fit, and speed, it is concluded that using a spherical pipeline cleaner for cleaning operations can achieve the best cleaning effect and efficiency.

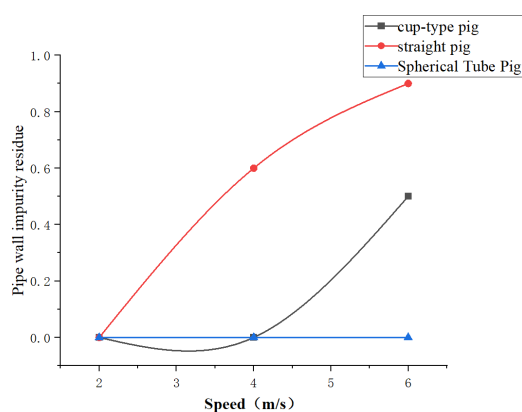


Figure 10. Comparison of the residual impurities on the pipe wall after cleaning with the pig at different running speeds.

7. Funding

This work was supported in part by the Sichuan Science and Technology Program (2023YFH0102, 2022YFH0119 and 2023NSFSC1980), in part by the scientific research starting project of SWPU (No. 2021QHZ040), and in part by the National Natural Science Foundation of China under Grant 52005269 and Grant 51805443.

References

- [1] Wang Y, Fan S, Lang X. Reviews of gas hydrate inhibitors in gas-dominant pipelines and application of kinetic hydrate inhibitors in China[J]. Chinese Journal of Chemical Engineering, 2019, 27(9): 2118-2132.
- [2] Ke W, Chen D. A short review on natural gas hydrate, kinetic hydrate inhibitors and inhibitor synergists[J]. Chinese Journal of Chemical Engineering, 2019, 27(9): 2049-2061..
- [3] dos Santos J P L, Lobato A K C L, Moraes C, et al. Comparison of different processes for preventing deposition of elemental sulfur in natural gas pipelines: A review[J]. Journal of Natural Gas Science and Engineering, 2016, 32: 364-372.

- [4] Quarini J, Shire S. A review of fluid-driven pipeline pigs and their applications[J]. Proceedings of the Institution of Mechanical Engineers, Part E: Journal of Process Mechanical Engineering, 2007, 221(1): 1-10.
- [5] SHORT G C. Conventional pipeline pigging technology: part 1-challenges to the industry [J]. Pipes and Pipelines International, 1992, 37(3): 8-11.
- [6] Lino A C F, Pereira F B. Developing techniques, facilities for deepwater flowline pigging[J]. Pipe Line & Gas Industry, 1995, 78(8): 31-35.
- [7] Mendes P R S, Braga A M B, Azevedo L F A, et al. Resistive force of wax deposits during pigging operations[J]. 1999.
- [8] Wang Q, Sarica C, Volk M. An experimental study on wax removal in pipes with oil flow[J]. Journal of Energy Resources Technology, 2008, 130(4).
- [9] WANG Wenda. Study on the wax stripping law in the pigging process of crude oil pipe [D] (in Chinese). Beijing: China University of Petroleum (Beijing), 2016.
- [10] Liu Jianlin et al. Interference calculation of foam pigging and its effect on pigging effect[J](in Chinese). Journal of China University of Petroleum(Edition of Natural Science), 2021, 45(02):111-119.
- [11] Borregales M A, Ensalsado R, Asuaje M. CFD Analysis of phenomena attributed to pigging run in a straight pipeline [C]//ASME International Mechanical Engineering Congress and Exposition. American Society of Mechanical Engineers, 2014, 46545: V007T09A082.
- [12] Jaimes Parilli D, Blanco A, García J. Influence of PIG Mass, Launching Time and Turbulence Model on 3-D CFD Transient Simulation of PIG Motion[C]//ASME International Mechanical Engineering Congress and Exposition. American Society of Mechanical Engineers, 2016, 50619: V007T09A077.
- [13] Jaimes Parilli D, Loaiza N, Garcia J, et al. 3-D Transient CFD Modeling of Pig Motion[C]//International Pipeline Conference. American Society of Mechanical Engineers, 2016, 50275: V003T04A007.
- [14] Pereira E L L, Deschamps C J, Ribas F A. Performance analysis of reciprocating compressors through computational fluid dynamics[J]. Proceedings of the Institution of Mechanical Engineers, Part E: Journal of Process Mechanical Engineering, 2008, 222(4): 183-192.
- [15] Noh W F. CEL: A time-dependent, two-space-dimensional, coupled Eulerian-Lagrange code[R]. Lawrence Radiation Lab., Univ. of California, Livermore, 1963.
- [16] Faizan M, Pati S, Randive P R. Effect of non-uniform heating on conjugate heat transfer performance for nanofluid flow in a converging duct by a two-phase Eulerian-Lagrangian method[J]. Proceedings of the Institution of Mechanical Engineers, Part E: Journal of Process Mechanical Engineering, 2022, 236(2): 414-424.
- [17] Sillem A. Feasibility study of a tire hydroplaning simulation in a monolithic finite element code using a coupled Eulerian-Lagrangian method[J]. Delft university of technology, 2008.